

# $N$ –site-lattice analogues of $V(x) = ix^3$

Miloslav Znojil

Nuclear Physics Institute ASCR,  
250 68 Řež, Czech Republic  
e-mail: znojil@ujf.cas.cz

## Abstract

A discrete  $N$ –level alternative to the popular imaginary cubic oscillator is proposed and studied. As usual, the unitarity of evolution is guaranteed by the introduction of an *ad hoc*, Hamiltonian-dependent inner-product metric, the use of which defines the physical Hilbert space and renders the Hamiltonian (with real spectrum) observable. Due to the simplicity of our model of dynamics the construction of the set of eligible metrics is shown tractable by non-numerical means which combine the computer-assisted algebra with the extrapolation and/or perturbation techniques.

## KEYWORDS

cryptohermitian discrete Schroedinger equations; deformed imaginary cubic oscillators; exceptional points; spectral topology; critical exponents; operators of metric; extrapolations; Fibonacci numbers;

# 1 Introduction

Many measured spectra of energies may be interpreted as excitations of a quasiparticle. The simplest fits of such a type employ the elementary one-dimensional differential Schrödinger equation

$$-\frac{d^2}{dx^2}\psi_n(x) + V(x)\psi(x) = E_n\psi_n(x) \quad \psi(\pm\Lambda) = 0, \quad \Lambda \leq \infty \quad (1)$$

containing a real potential  $V(x)$ . In more sophisticated models, potential  $V(x)$  may even be allowed complex, provided only that the spectrum itself remains real (cf. reviews [1, 2, 3, 4] for details).

Whenever  $V(x) \neq V^*(x)$ , the reality of the spectrum may be fragile and sensitive to perturbations [5]. A remarkable exception emerges with the robustly real spectra generated by many potentials with the property  $V(x) = V^*(-x)$  called, in the literature,  $\mathcal{PT}$ -symmetry [2] alias parity-pseudo-Hermiticity [3] alias Krein-space-Hermiticity [6].

In the early studies of this remarkable mathematical phenomenon the attention of the authors has mainly been restricted to the imaginary cubic oscillator example  $V(x) = V^{(IC)}(x) = ix^3$  modified, possibly, by some other, asymptotically subdominant terms (cf., e.g., papers by Caliceti et al [7], by Alvarez [8] or by Bender et al [9, 10] and several further authors [11]). In what follows we shall mainly feel inspired by this choice of  $V(x)$  as well.

The essence of our present message will lie in the recommendation of a drastic simplification of the necessary mathematics. In a way explained in section 2 this will be achieved by means of the replacement of the differential Schrödinger equation (1) by its discrete, difference-equation analogue. A few simplest illustrations will be then added in section 3 where the discretization of the coordinate will be shown to facilitate the study of the reality (i.e., in principle, observability) of the spectrum.

The desirable flexibility of our present discrete simulation of the dynamical energy spectra will be shown achieved by a supplementary one-parametric deformation of the potential resembling slightly the influential proposal of deformation  $ix^3 \rightarrow (ix)^{3+\delta}$  by Bender and Boettcher [10]. The details will be described in section 4. The subsequent section 5 will then recall the known theory and explain some of its details via the simplest possible example with  $N = 2$ . In sections 6 – 8 we shall finally present some applications of this theory to the models with  $N = 4$ ,  $N = 6$  and general  $N = 2K \geq 8$ , respectively. Section 9 is summary.

## 2 Discrete Schrödinger equations

The spectrum of many Krein-space-Hermitian Hamiltonians  $H \neq H^\dagger$  has been found robustly real and bounded below [10, 12, 13]. In the spirit of the general theory as outlined, first, by Scholtz et al [14], one can conclude that the apparent non-Hermiticity is “false” and that it may be reinterpreted as a mere consequence of an inappropriate choice of the Hilbert-space representation  $L^2(\mathbb{R}) \equiv \mathcal{H}^{(F)}$ . Hence, the abstract remedy is straightforward and

lies in an interpretation-mediating transition to a “standard” Hilbert space of states  $\mathcal{H}^{(S)}$  [4].

In the practical applications of such a theoretical scheme the original vector space is usually being endowed with a general, *non-local* inner product,

$$\langle \psi | \phi \rangle^{(S)} = \int \int \psi^*(x) \Theta(x, y) \phi(y) dx dy \equiv \langle \psi | \Theta | \phi \rangle^{(F)}, \quad \Theta = \Theta^\dagger > 0. \quad (2)$$

For the one-dimensional imaginary cubic oscillator Hamiltonians

$$H = H^{(IC)}(\lambda) = -\nabla^2 + i\lambda x^3 + \dots$$

(where the dots may represent certain asymptotically subdominant terms) the first constructions of the necessary “standard metric” were perturbative. They appeared in 2003 [15] and in 2004 [16], yielding the metric operator

$$\Theta = \Theta(H^{(IC)}) = \exp(-Q_1\lambda - Q_2\lambda^2 - \dots) \quad (3)$$

with  $Q_1(x, y) = ixy(x^2 + y^2)\text{sign}(x - y)/2^4$ , etc. In the light of the well known fact that the assignment of the metric  $\Theta$  to a given Hamiltonian  $H$  cannot be unique in general [14, 17], additional, multiparametric metrics  $\Theta_{(c_1, c_2, \dots)}(H^{(IC)})$  were further found and constructed in Refs. [16] and [18].

The latter calculations proved facilitated by an additional assumption of the absence of a nontrivial fundamental length  $L > 0$  in the theory. Unfortunately, the *presence* of such a preassigned length scale has been found essential in Ref. [19] where an extension of the formalism to the scattering dynamical regime has been proposed. Naturally, under the assumption of the presence of a fixed length scale  $L > 0$ , additional ambiguities will emerge in the metrics. In the differential-operator models their explicit specification might prove prohibitively difficult (cf., e.g., Ref. [20] or section 6 of Ref. [18] for related comments).

We shall address here this problem while accepting the discretization strategy of Ref. [19]. In the way based on the use of equidistant, Runge-Kutta grid-point coordinates  $x_k = -\Lambda + kh$ ,  $k = 0, 1, \dots, N+1$ , the ordinary differential Schroedinger Eq. (1) will be replaced by its discrete version

$$-\frac{\psi(x_{k-1}) - 2\psi(x_k) + \psi(x_{k+1}))}{h^2} + V(x_k)\psi(x_k) = E\psi(x_k) \quad (4)$$

with  $x_{N+1} = \Lambda$  (i.e.,  $h = 2\Lambda/(N+1)$ ) and with the Dirichlet boundary conditions

$$\psi(x_0) = \psi(x_{N+1}) = 0. \quad (5)$$

This leads to the reduction of the problem to the (numerical) determination of the  $N$ -plets of eigenvalues  $E_j^{(N)}$ ,  $j = 1, 2, \dots, N$ , i.e., of the eigenvalues  $\varepsilon_j := h^2 E_j^{(N)} \in (0, 4)$  of the re-scaled,  $N$ -dimensional Hamiltonians

$$H^{(N)} = \begin{pmatrix} 2 + h^2 V(x_1) & -1 & & & \\ -1 & 2 + h^2 V(x_2) & -1 & & \\ & -1 & 2 + h^2 V(x_3) & \ddots & \\ & & \ddots & \ddots & -1 \\ & & & -1 & 2 + h^2 V(x_N) \end{pmatrix}. \quad (6)$$

We intend to make use of this definition of the Hamiltonian in the whole rest of our present paper. Nevertheless, before we fully concentrate on its bound-state aspects and consequences, let us make a small detour and point out that our present acceptance of the Dirichlet boundary conditions (5) is in fact just one of the two basic alternative options which are at our disposal in the phenomenologically oriented applications. In a very close parallel to the continuous cases, these boundary conditions could have been replaced, even in the Runge-Kutta-discretized models, by the alternative scattering scenario.

In the latter context, one might feel discouraged by a threatening technical difficulty connected with the necessity of working with the infinite-dimensional matrices. Still, there exist tricks which enable us to avoid these difficulties by assuming that our interaction  $V(x)$  in Eq. (6) is just short-ranged (plus, admissibly, non-Hermitian and non-local). For more details and/or for an explicit constructive illustration of such an alternative possibility, interested readers might consult, e.g., Ref. [21].

### 3 The series of one-parametric Hamiltonians

Let us pick up the potential  $V(x_j) = ix_j^3$  and insert it in Eq. (6). Once we abbreviate  $a = h^5/8$  we obtain the following one-parametric sequence of Hamiltonians

$$H^{(2)}(a) = \begin{pmatrix} 2 - ia & -1 \\ -1 & 2 + ia \end{pmatrix}, \quad H^{(3)}(a) = \begin{pmatrix} 2 - 8ia & -1 & 0 \\ -1 & 2 & -1 \\ 0 & -1 & 2 + 8ia \end{pmatrix},$$

$$H^{(4)}(a) = \begin{pmatrix} 2 - 27ia & -1 & 0 & 0 \\ -1 & 2 - ia & -1 & 0 \\ 0 & -1 & 2 + ia & -1 \\ 0 & 0 & -1 & 2 + 27ia \end{pmatrix}, \dots \quad (7)$$

The first element  $H^{(2)}(a)$  of this series is particularly elementary. For this reason it has also been chosen and studied in the methodical part of Ref. [15] (cf. its section II. B).

For the sake of brevity we shall restrict our attention to the matrices with even dimension  $N = 2K$ . Thus, in the simplest case with  $K = 1$  one encounters the compact and explicit energy formula  $\varepsilon_{1,2} = 2 \mp \sqrt{1 - a^2}$ . Such a two-level spectrum remains real iff  $a \in (-1, 1)$ , forming a circle in the energy-coupling plane. The similar formulae and conclusions may be also obtained at the next few  $K$ s.

The first nontrivial sample of the  $a$ -dependence of the spectrum may be obtained at  $N = 4$ . Its shape is displayed in Fig. 1. The algebraic representation of these energies is elementary,

$$\varepsilon_{1,2,3,4} = 2 \mp 1/2 \sqrt{6 - 1460 a^2 \pm 2 \sqrt{529984 a^4 - 1680 a^2 + 5}}.$$

One can easily deduce that these energies remain real for  $a \in (-\alpha^{(4)}, \alpha^{(4)})$  where  $\alpha^{(4)} = 1/2 - 1/18 \sqrt{69} \approx 0.0385208965$ .

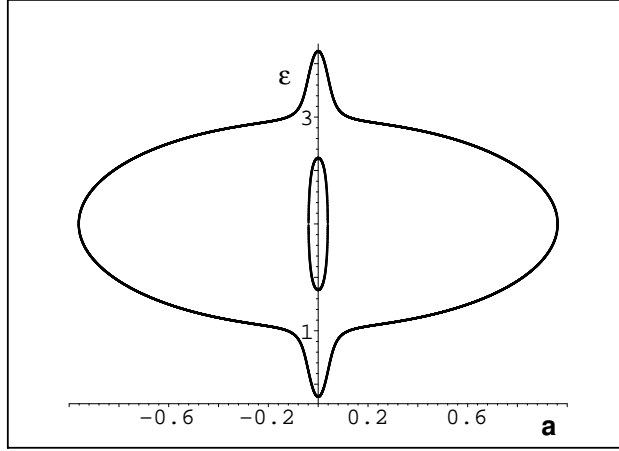


Figure 1: The parameter-dependence of the *real-energy* eigenvalues  $\varepsilon(a)$  of the toy Hamiltonian  $H^{(4)}(a)$  [= the third item in the list (7)]. In topological language, this spectral locus is formed of the two (deformed) cocentric circles.

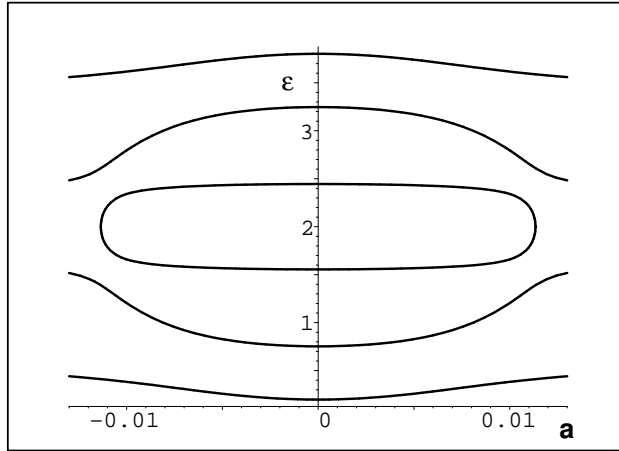


Figure 2: Same as Figure 1, at the next even dimension  $N = 6$ . The spectral locus is formed of the three (deformed) cocentric circles (note that the horizontal axis is rescaled).

Numerical difficulties start emerging at  $N = 6$  since the purely algebraic representation of the spectrum requires the use of Cardano formulae in which the imaginary numerical errors occur and survive, disappearing only in the infinite-precision arithmetics. Still, the more or less routine control of precision enables us to conclude that the  $N = 6$  spectrum remains real iff  $a \in (-\alpha^{(6)}, \alpha^{(6)})$ . The approximate numerical value of  $\alpha^{(6)} \approx 0.011344897$  may be read out of Fig. 2 and/or of its appropriate systematic magnifications.

We may notice that at  $N = 4$  and  $N = 6$  the ends  $\pm\alpha^{(4,6)}$  of the interval of the reality of the whole spectrum are determined by the confluence (followed by the complexification) of a single pair of energies (lying in the middle of the spectrum). Both of these models are exceptional. Starting from  $N = 8$  the pattern gets changed and we encounter the less trivial  $a$ -dependence of the energies  $\varepsilon(a)$  characterized by the fragility and confluence of the *two* pairs of

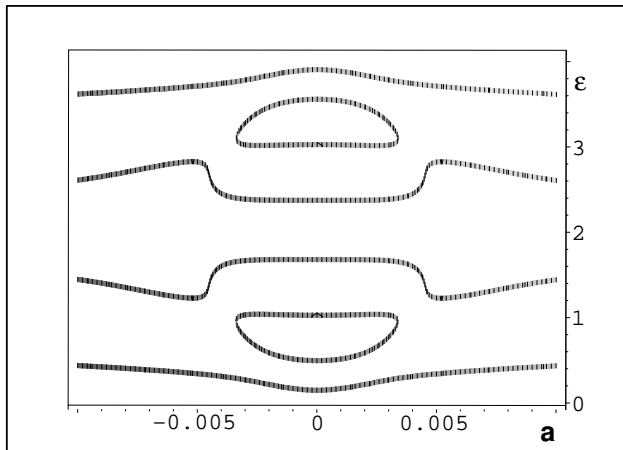


Figure 3: The next item in the series of Figures 1 and 2. The horizontal axis is further rescaled and the  $N = 8$  spectral locus gets nontrivial. In topological terms, it becomes composed of the vertical array of the three circles, all being circumscribed by the fourth one.

Table 1: The exceptional-point coordinates of the loss of reality of the first and second excited state ( $z = 3$ ).

dimension $N$	critical parameter $\alpha$	twice-degenerate energy $\varepsilon_2(\alpha) = \varepsilon_3(\alpha)$
2	1	2
4	$1/2 - \sqrt{69}/18$	2
6	0.011344897	2
8	0.003383828	0.9285
10	0.001246890	0.6194
12	0.000543788	0.4438
14	0.000266880	0.3335
$\vdots$	$\vdots$	$\vdots$

the energy levels (cf. Fig.3).

The latter form of the loss of reality is generic. The  $N = 14$  sample of the spectrum as displayed in Fig. 4 elucidates some details. In the picture we see that the spectral locus (i.e., the set of all of the real energies  $\varepsilon_j(a)$  with  $a \in (-\infty, \infty)$  and  $j = 1, 2, \dots, N$ ) preserves the form which remains up-down and left-right symmetric. During the growth of  $N = 2K$  the graphical analysis of the model remains feasible and reveals a steady shrinking of the interval of the parameters  $a$  for which the spectrum remains real.

A quantitative account of the latter phenomenon is presented in Table 1. The inspection of this Table reveals that the presence of the fundamental-length parameter  $\alpha^{(N)}$  (= a maximum of admissible  $as$ , decreasing with  $N$ ) in our present model implies an obvious mismatch between the large- $N$  spectrum (with a very small interval of reality) and the robustly real spectrum which has been proved to exist in the differential-equation limit  $N = \infty$  [12].

An explanation of the paradox is twofold. Firstly, the enormously small

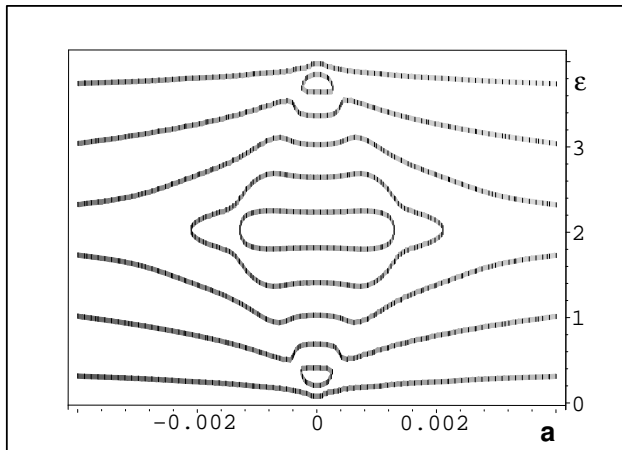


Figure 4: A sample of a “multilevel descendant” of the preceding Figures. At  $N = 14$  we see a “generic” pattern in which we encounter  $(N - 6)/2$  concentric circles plus a single “top” and single “bottom” circle, all being circumscribed by the “biggest” last circle. The interval of the reality of *all* of the eigenvalues  $\varepsilon(a)$  of the toy Hamiltonian  $H^{(14)}(a)$  has further shrunk.

magnitude of  $a = \mathcal{O}(h^5)$  makes the comparison only sensible in the limit  $a \rightarrow 0$  (in this sense, the spectrum of the discrete model remains robustly real at all  $N$ ). Secondly, at any finite dimension  $N < \infty$  even the role of the Runge-Kutta error terms  $\mathcal{O}(h^4) \gg \mathcal{O}(a)$  remains unspecified. Whenever the limit of  $N \rightarrow \infty$  is considered, this observation offers another argument against drawing any  $N \rightarrow \infty$  implications from the observations made at the finite  $N$  and nonvanishing values of  $a$  in our models.

## 4 The series of two-parametric Hamiltonians

In the examples of the preceding section we encounter another suspicious feature even at any fixed and finite dimension  $N = 2K$ . Indeed, the critical left and right points  $a = \pm\alpha^{(2K)}$  of the loss of the reality of the spectrum seem to be exclusively connected with the confluence of the first and second lowest excited states  $\varepsilon_2$  and  $\varepsilon_3$  or, symmetrically, of their equally “privileged” mirror partners  $\varepsilon_{N-2}$  and  $\varepsilon_{N-1}$ .

In what follows we shall explain this apparent privilege as an artifact caused by the too specific choice of the potential. The constructive explanation will be based on a rescaling of the interaction  $V(x) = ix^3$ . Its third power term will be replaced by an odd function  $f_{(z)}(x) \sim \text{sign}(x)x^z$  with a real exponent  $z \in \mathbb{R}$ . As long as our models are discrete, we need not follow the conventional wisdom and require that the functions  $f_{(z)}(x)$  are analytic.

Thus, we arrive at the family of two-parametric Hamiltonians  $H^{(2K)}(a, z) =$

$$\begin{bmatrix} 2 - i a (2K - 1)^z & -1 & 0 & \dots & \dots & 0 \\ -1 & \ddots & \ddots & \ddots & & \vdots \\ 0 & \ddots & 2 - i a 3^z & -1 & 0 & \\ \vdots & \ddots & -1 & 2 - i a & -1 & 0 \\ & & 0 & -1 & 2 + i a & -1 & \ddots & \vdots \\ & & & 0 & -1 & 2 + i a 3^z & \ddots & 0 \\ \vdots & & & & \ddots & \ddots & \ddots & -1 \\ 0 & \dots & & \dots & 0 & -1 & 2 + i a (2K - 1)^z \end{bmatrix}. \quad (8)$$

We shall see below that such a class of discrete deformations

$$V(x) = ix^3 := if_{(3)}(x) \rightarrow V(x) = if_{(z)}(x)$$

may be made responsible for the emergence of a full range of possible complexification patterns. In the language of dynamics and phenomenology, we shall show below that the emergence of the new parameter  $z$  in models (8) renders them tractable as offering a certain *complete* set of alternative, tuneable topological features of the spectrum. In this sense our present *complex-interaction* models may be perceived as complementing the recent attempts of achieving a topology-related tuning of spectra via a *non-locality* of real  $V(x)$  [22] or, alternatively, via a *nontriviality* of the “coordinates”  $x$  living, say, on real closed loops [23] or on certain specific multisheeted complex curves [24].

#### 4.1 Spectral loci $\varepsilon^{(N,z)}(a)$ : the $N = 4$ prototype

As we indicated, the key source of interest in our two-parametric models  $H^{(2K)}(a, z)$  should be seen in the enhancement of the flexibility of the  $a$ -dependence of the spectrum. Moreover, one can expect that the choice of  $z$  might re-assign the role of the most fragile levels all along the spectrum.

In an expected verification of these hypotheses, let us now select  $N = 4$  and turn attention to the two-parametric Hamiltonian

$$H^{(4)}(a, z) = \begin{bmatrix} 2 - i a 3^z & -1 & 0 & 0 \\ -1 & 2 - i a & -1 & 0 \\ 0 & -1 & 2 + i a & -1 \\ 0 & 0 & -1 & 2 + i a 3^z \end{bmatrix}. \quad (9)$$

Due to the simplicity of such a generalization of the purely cubic discrete model (7) it may be easily shown, graphically, that the spectral pattern displayed in Fig. 1 does not change too much when the exponent-parameter  $z$  starts to be different from three. Indeed, with the steady growth of  $z > 3$  one merely reveals that the small internal ellipse in the picture of Fig. 1



will shrink. In a numerical test performed at  $z = 25$ , for example, we still recognized the existence of this inner ellipse but only on the scale of  $a$ s of the order of magnitude of  $10^{-12}$ .

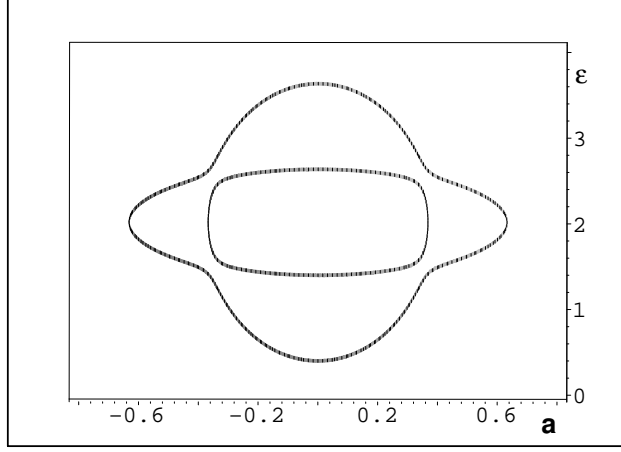


Figure 5: The  $a$ -dependence of the real eigenvalues  $\varepsilon(a) = \varepsilon^{(N,z)}(a)$  of the two-parametric toy Hamiltonian  $H^{(N)}(a, z)$  at  $N = 4$  [cf. Eq. (9)]. Slightly above a critical value of  $z = 85/64 \sim 1.328125 > z_{critical}$ , the pattern is still formed by the two cocentric circles.

In the opposite direction of the change, i.e., with the decrease of  $z$  below three the internal ellipse broadens. From the inspection of Fig. 5 we may deduce that slightly below the value of  $z = 85/64$  the internal ellipse must ultimately touch the external deformed circle. At this moment the whole spectral locus will acquire the form of the two intersecting ellipses. After the further small decrease of  $z$  we recognize a qualitatively (i.e., topologically) new pattern, the form of which is sampled, at the next rational numerical value of  $z = 84/64$ , in Fig. 6.

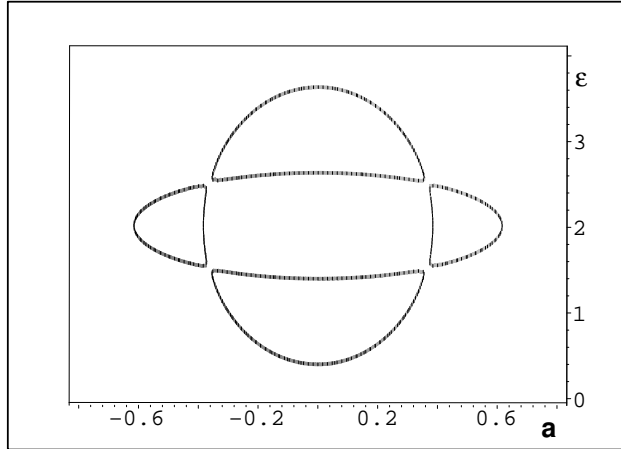


Figure 6: The breakdown of the cocentric-circles pattern of Figure 5 when the value of  $z$  dropped just slightly below the critical value,  $z = 84/64 = 1.3125 \lesssim z_{critical}$ .

With the continuing decrease of  $z$  we witness a quick shrinking of the two spurious large- $|a|$  intervals of partial reality of the spectrum. Both of

them are centered around  $|a| = 1/2$  while leaving still the two levels real (cf. Fig. 7 where we choose  $z = 81/64 = 1.265625$ ). We also repeated the same graphical analysis below the latter value of the exponent. We revealed that quickly, both the anomalous partial-reality intervals have got empty and disappeared.

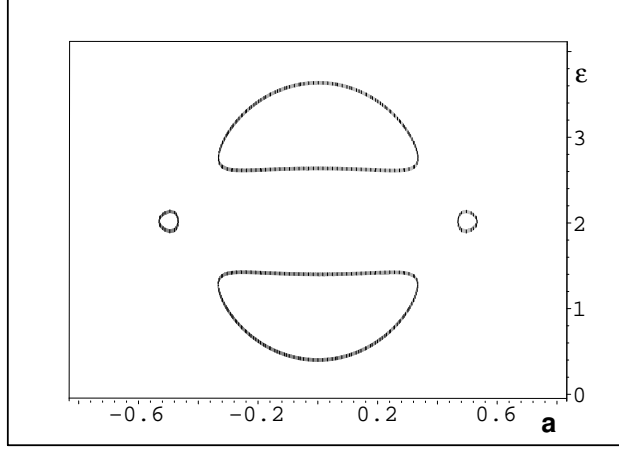


Figure 7: The “evolution-to-disappearance” of the left and right “anomalous” topological circles of Figure 6 at  $z = 81/64 = 1.265625 < z_{critical}$ . During the further decrease of  $z$ , just the real spectral locus composed of the horizontal array of two nonintersecting (deformed) circles will survive.

Needless to add that the further steady decrease of  $z$  already keeps the “two-oval” topology of the spectral pattern unchanged. We checked this empirical rule in the exactly tractable limit of  $z = 0$ . In this limit the quadruplet of the energies acquires the compact form

$$\varepsilon(a) = 2 \pm 1/2 \sqrt{6 - 4a^2 \pm 2\sqrt{-16a^2 + 5}}, \quad z = 0.$$

One can strictly deduce that this spectrum remains real iff  $a \in (-\sqrt{5}/4, \sqrt{5}/4)$ .

## 4.2 Sequences of rearrangements: the $N = 8$ prototype

The straightforward generalization of Eq. (9) to any dimension yields the  $N$  by  $N$  matrix  $H^{(2K)}(a, z)$  of Eq. (8). The related geometric shapes of the spectra just generalize the  $N = 4$  pattern. At any  $N = 2K$  and at all of the sufficiently large exponents we revealed that the picture of the real spectral locus in the  $(\varepsilon, a)$ -plane remains topologically equivalent to the set of cocentric circles. At  $N = 8$  and  $z = 9/2$  and  $z = 8/2$ , the respective Figs. 8 and 9 offer the two characteristic samples of the evolution of the large-exponent spectrum with the decrease of the exponent  $z > z_{first\ critical}^{(2K)}$ .

In a series of graphical experiments using the smaller and smaller rational exponents  $z$  we were able to keep the numerical precision under good control. We discovered that  $z_{first\ critical}^{(8)} \lesssim 4$ . Below this value though safely above  $z_{second\ critical}^{(8)} \gtrsim 12/4$  (cf. Fig. 3 above), one encounters the new topological pattern sampled by Figs. 10 or 11.

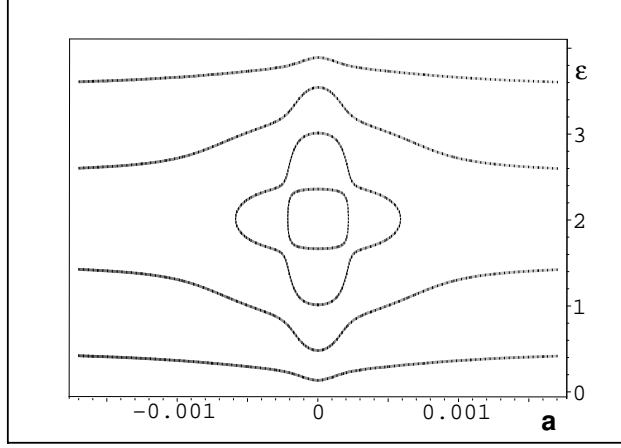


Figure 8: For the less elementary matrix  $H^{(2K)}(a, z)$  of Eq. (8) with  $K = 4$ , the spectral locus remains composed of the four concentric (deformed) circles at all the sufficiently large exponents  $z$ . This pattern is sampled here at  $z = 9/2 > z_{first\ critical}^{(8)}$ .

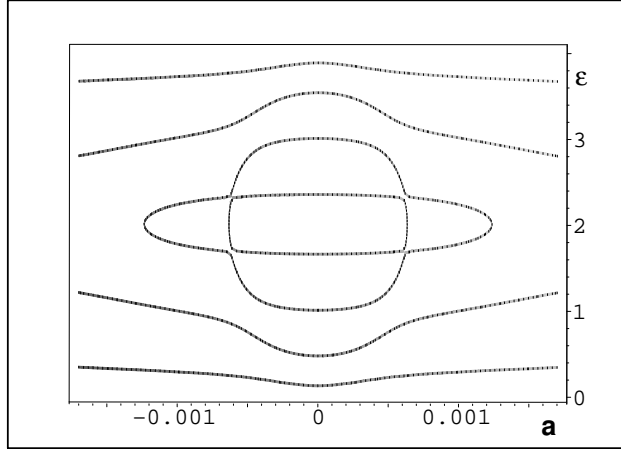


Figure 9: The topology of Figure 8 is not yet changed in the “close-to-crossing” case of  $z = 8/2 \gtrsim z_{first\ critical}^{(8)}$ .

The corresponding second-pattern regime may further be split in two stages. In the initial stage of the decrease of  $z$  there survive two large- $|a|$  anomalies which quickly shrink and, not too far below the first critical value of the exponent, disappear. In the final stage of the decrease the picture of the whole real spectral locus in the  $(\varepsilon, a)$ -plane acquires the “fully canonical” form of the two cocentric (deformed) circles with a vertically ordered pair of non-intersecting circles (or rather deformed ellipses) inside.

The next, second change of the topological pattern has been spotted to occur between  $z = 13/4$  (cf. Fig. 11) and  $z = 7/4$  (cf. Fig. 12) while the third change certainly follows between  $z = 7/4$  and  $z = 6/4$  (cf. Fig. 13). Ultimately, the list of the topological changes of the  $N = 8$  spectral loci is made complete during the transition between  $z = 6/4$  and  $z = 1/2$  (cf. Fig. 14). One arrives at the other, small-exponent extreme in which the spectral locus stays unchanged and topologically equivalent to a vertically ordered quadru-

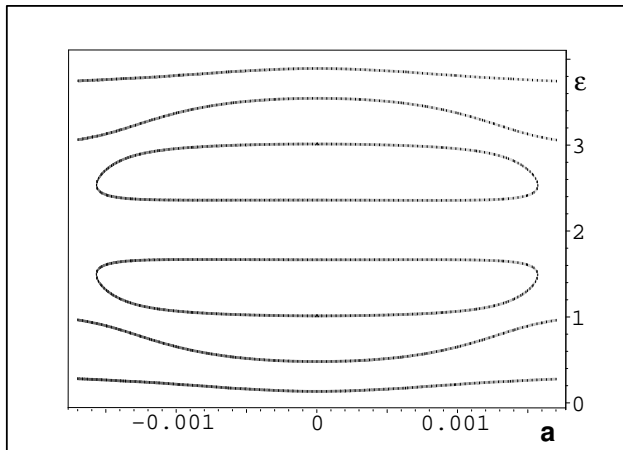


Figure 10: The innermost circles of Figures 8 or 9 are being replaced by their horizontal array at  $z = 14/4 \in (z_{\text{second critical}}^{(8)}, z_{\text{first critical}}^{(8)})$ . Notice that we moved safely below  $z_{\text{first critical}}^{(8)}$  so that the temporary left and right real-eigenvalue anomalies have already (and very quickly) disappeared.

plet of separate deformed circles.

The results of our calculations aimed at a more precise determination of the numerical values of the quadruplet of critical exponents at  $N = 8$  are summarized in Table 2. In order to make these calculations feasible, we were forced to give up the full control of the numerical precision. For this reason, Table 2 does not contain any estimates of the error bars so that even the last digits in our numerical values of the critical exponents  $z$  should not be taken for granted.

Marginally, let us add that, strictly speaking, our present list of the five critical points might have been complemented not only by the list of certain “secondary critical” points  $\tilde{z}$  (marking the disappearance of the above-mentioned left and right partial-reality intervals in the anomalous, large- $|a|$  dynamical regime) but also by the list of certain “tertiary critical” points  $\tilde{\tilde{z}}$  at which these left and right anomalies change from “containing” to “not-containing” an even narrower four-level-reality subinterval.

The readers who would be interested in the similar subtleties might consult the results of this type as obtained, e.g., in Ref. [22]. In the present context, a sample of such an analysis has merely been performed in the small-exponent regime with  $z \geq 0$  where we found  $z_{\text{fourth critical}}^{(8)} \approx 1.0358$ .

In this setting the unchanged topology without anomalies has been only demonstrated to exist in the slightly smaller interval of  $z \in (-\infty, \tilde{z})$  with  $\tilde{z} \approx 1.033$ . Within the latter, anomaly-free interval, the variations of  $z$  still preserved the strict reality just along the four non-intersecting ellipses, more and more deformed and all the time located in a vertical arrangement. In the adjacent, very short interval of  $z \in (1.033, 1.0358)$  there emerged the left and right anomaly as sampled, at  $N = 4$ , in Fig. 7.

At the fourth critical value of  $z \approx 1.0358$  we obtained, in accord with our expectations, the transitional intersection of ellipses as sampled, at  $N = 4$ , in Fig. 6. We can conclude that our numerical study of the  $N = 8$  model confirmed that when we ignore the partial-reality anomalies as inessential

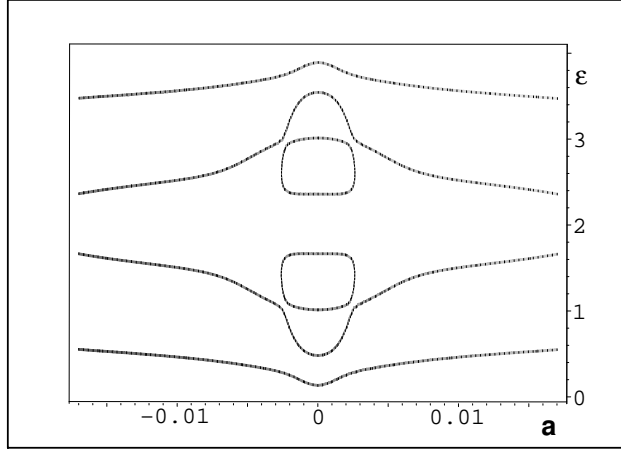


Figure 11: The topology-preserving deformation of Figure 10 during the further decrease of the exponent to  $z = 13/4 \gtrsim z_{second\ critical}^{(8)}$  (notice also the change of scale of  $a$ ).

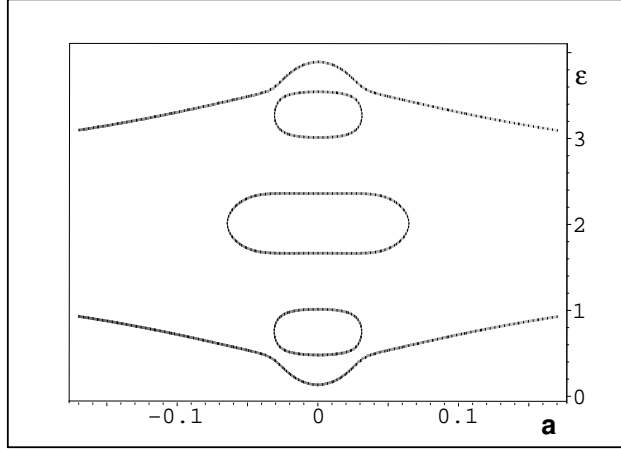


Figure 12: The next change of topology of the spectral locus as sampled at  $z = 7/4 > z_{third\ critical}^{(8)}$ .

for the fully unitary quantum systems, the range of the exponents  $z \geq 0$  (or rather  $z > -\infty$ ) splits into five subintervals on which the spectral loci  $\varepsilon(a)$  become topologically non-equivalent. The exhaustive and fully explicit description of these  $N = 8$  topologies is also given in Table 2.

### 4.3 Rearrangements: Fibonacci-sequence connection

Fig. 8 may be perceived as the inessential  $N = 8$  sophistication of the  $N = 4$  pattern of Fig. 5. Similarly, Fig. 9 recycles the structure which is shown in Fig. 6, while Fig. 10 may be read as paralleling Fig. 7. The generic  $N > 6$  pattern only starts emerging, at  $N = 8$ , during the transition from Fig. 11 to Fig. 12. It is characterized by the *two* parallel confluences of energy pairs at the critical exponent  $z_{second\ critical}$ . The similar phenomenon occurs at all of the further critical points, viz., at the remaining two topology-changing transitions from Fig. 12 to Fig. 13 and from Fig. 13 to Fig. 14.

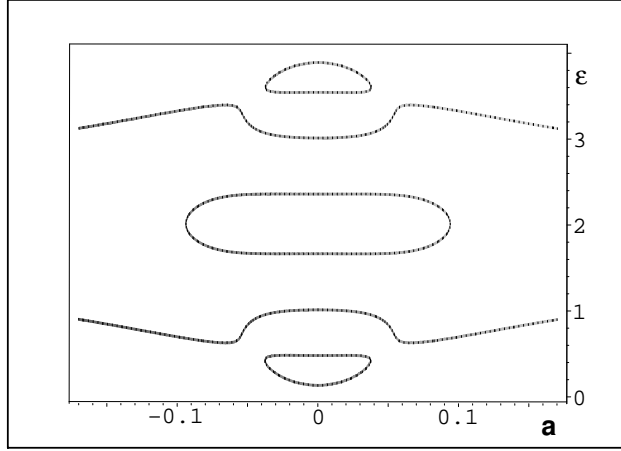


Figure 13: The next topological arrangement of the spectral locus sampled at  $z = 6/4 \in (z_{third\ critical}^{(8)}, z_{fourth\ critical}^{(8)})$ .

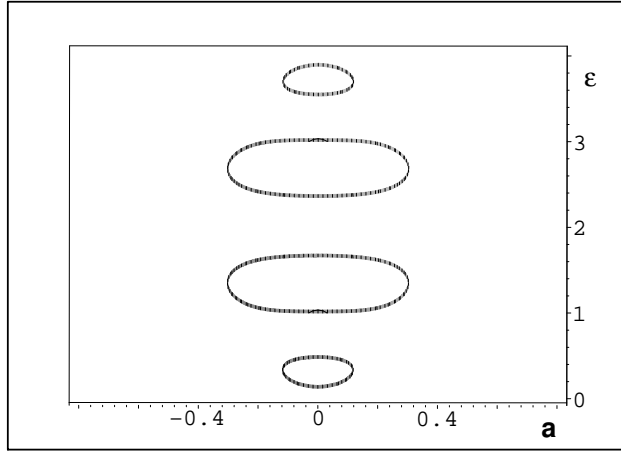


Figure 14: The ultimate, “small-exponent” topology which is sampled here at  $z = 1/2$  but which is exhibited by any spectral locus  $\varepsilon(a)$  of matrix (8) at  $K = 4$  and any real  $z < z_{fourth\ critical}^{(8)}$ .

At any higher dimension  $N = 2K$  the similar sequence of changes of topology can be assigned a fully systematic description. Thus, once we choose any  $N$  and assume the complete knowledge of the set  $\mathcal{T}_N$  of all of the related spectral-locus arrangements (consisting of the  $K$ -plets of deformed circles) which are topologically non-equivalent, we may contemplate a constructive transition to the next dimension  $N' = 2K + 2$ . In the first step we build the first subset  $\mathcal{F}_{N'}$  of new schemes  $\mathcal{T}_{N'}$  as the set of elements of the old set  $\mathcal{T}_N$  which are merely encircled by an additional, single outer (deformed) circle.

The construction of  $\mathcal{T}_{N'} = \mathcal{F}_{N'} \oplus \mathcal{S}_{N'}$  may be then completed by the discovery of the one-to-one correspondence of the second part  $\mathcal{S}_{N'}$  of the new set of schemes to the “one step older” set  $\mathcal{T}_{N''}$  where  $N'' = 2K - 2$ . Each of the “older” elements only has to be complemented by the *pair* of the single upper and the single lower additional (deformed) circles, indeed.

In the enumeration of the complete sets of non-equivalent patterns by induction, it is now sufficient to verify that the numbers  $\#\mathcal{T}_{2K}$  of the elements

Table 2: The five intervals of exponents yielding topologically non-equivalent real spectral loci  $\varepsilon(a)$  at  $N = 8$ .

the graph of $\varepsilon_j = \varepsilon_j(a)$ , $j = 1, 2, \dots, 8$	illustration	interval
four cocentric (deformed) circles	Figs. 8, 9	$z \in (3.982, \infty)$
two in vertical array, encircled by two	Figs. 10, 11	$z \in (3.178, 3.982)$
three in vertical array, encircled by one	Fig. 12	$z \in (1.630, 3.178)$
vertical, but the middle pair cocentric	Fig. 13	$z \in (1.0358, 1.630)$
four (deformed) circles in vertical array	Fig. 14	$z \in (-\infty, 1.0358)$

of the sets  $\mathcal{T}_{2K}$  are equal to  $K$  for  $K = 1, 2, 3$ . Thus, we have proved

**Lemma 1.** *We have  $\#\mathcal{T}_{2K} = F_{K-1}$  where  $F_j$  is the  $j$ -th Fibonacci number.*

**Remark 1.** The sequence of Fibonacci numbers  $F_j$  is defined by recurrences  $F_j = F_{j-1} + F_{j-2}$  yielding  $\#\mathcal{T}_8 = 5$ ,  $\#\mathcal{T}_{10} = 8$ ,  $\#\mathcal{T}_{12} = 13$ , etc.

## 5 Interpretation

Usually [25] people decide to work in a fixed, specific Hilbert space  $\mathcal{H}^{(S)}$  and treat a given quantum system as physical if and only if its time evolution is unitary. Naturally, this is the strategy which does not change if the space  $\mathcal{H}^{(S)}$  proves endowed with a general, nontrivial metric  $\Theta = \Theta^\dagger > 0$  (i.e., with its inner product defined in terms of this metric, cf. Eq. (2) above). One still has to guarantee that every candidate for an operator of observable proves self-adjoint *with respect to this metric* [14].

For our present, manifestly non-Hermitian matrix representations  $H^{(N)}$  of the Hamiltonians (which will have to play the role of the generators of the *unitary* time evolution in  $\mathcal{H}^{(S)}$ ) we must guarantee their Hermiticity with respect to the given nontrivial metric. Such a form of nontrivial Hermiticity could be better called *cryptohermiticity* [4]. In the context of mathematics, such a condition is often being interpreted as the Dieudonné’s [26] “quasi-Hermiticity” constraint,

$$H^{(N)} = [H^{(N)}]^\dagger := \Theta^{-1} [H^{(N)}]^\dagger \Theta. \quad (10)$$

In the application of such an approach which is to be employed in what follows, we shall always start from a given matrix  $H^{(N)}$  and reconstruct the *ad hoc* metric (or metrics)  $\Theta = \Theta(H)$  via Eq. (10), treating this constraint as a linear algebraic set of equations for the matrix elements of the metric.

### 5.1 The simplest $N = 2$ illustration

For the most elementary,  $z$ -independent  $N = 2$  “input” Hamiltonian (cf. the first item in Eq. (7)), the solution of Dieudonné’s constraint (10) yields the complete, two-parametric family of the most general matrices of “output”

pseudometrics,

$$\Theta [H^{(N)}(a)] = \Theta [H^{(N)}(a)]_{(k,m)} = \begin{bmatrix} k & km - ika \\ km + ika & k \end{bmatrix}, \quad k, m \in \mathbb{R}. \quad (11)$$

Physical condition  $a \in (-1, 1)$  guaranteeing the reality of the energies must be complemented by the condition of positivity of the (two) eigenvalues

$$\theta = \theta_{\pm} = k \pm \sqrt{k^2 m^2 + k^2 a^2} > 0. \quad (12)$$

Only such a condition will open the possibility of using the corresponding pseudometric (11) as a metric in  $\mathcal{H}^{(S)}$  [14].

We see that  $k$  must be positive and larger than the square root. We may set  $a = \cos \beta \sin \gamma$  and  $m = \cos \beta \cos \gamma$  with, say,  $\beta \in (0, \pi)$  and  $\gamma \in (0, \pi)$  and  $-1 < \cos \beta < 1$ . This reparametrization leads to the final and most general positive definite and Hermitian metric

$$\Theta = \Theta \{H^{(2)}[a(\beta, \gamma)]\}_{[k, m(\beta, \gamma)]} = k \cdot \begin{bmatrix} 1 & e^{-i\gamma} \cos \beta \\ e^{i\gamma} \cos \beta & 1 \end{bmatrix} \quad (13)$$

which is never diagonal. As long as it contains free parameters, their choice will fix the inner product and, hence, it will specify the Hilbert space  $\mathcal{H}_{(\beta, \gamma)}^{(S)}$  of admissible states of the model. The choice of parameters  $\beta$  and  $\gamma$  will determine *both* the Hamiltonian  $H^{(2)}(a)$  and the metric  $\Theta_{(k, m)}^{(S)}$  (with, say,  $k = 1$ ), i.e., the true and complete *physical* contents of the theory.

## 5.2 Eligible observables

In our  $N = 2$  theory, *any* matrix  $\Lambda = \Lambda_{(\beta, \gamma)}^{(2)}$  representing an observable quantity must be self-adjoint in  $\mathcal{H}_{(\beta, \gamma)}^{(S)}$ , i.e. [4], we must have

$$\Lambda_{(\beta, \gamma)}^{\dagger} \Theta_{[k, m(\beta, \gamma)]} = \Theta_{[k, m(\beta, \gamma)]} \Lambda_{(\beta, \gamma)}. \quad (14)$$

This equation must be satisfied by the eligible representation matrices

$$\Lambda = \begin{bmatrix} G + ig & B + ib \\ C + ic & D + id \end{bmatrix}. \quad (15)$$

Naturally, Eq. (14) admits an arbitrary  $k$ -rescaling of  $\Theta \{H^{(2)}[a(\beta, \gamma)]\}$  and/or a similar trivial rescaling of  $\Lambda_{(\beta, \gamma)}$ . In terms of matrix elements one can easily check that this equation imposes four real constraints upon the eight free parameters in (15). This means that the  $N = 2$  family of available observables is four-parametric in general.

The details of the construction are left to the readers. We can only summarize that the three constraints are trivial and that they merely define quantities  $B$ ,  $C$  and the difference  $G - D$ . The remaining, fourth constraint acquires the form of a linear relation between sums  $c_{\Sigma} = b + c$  and  $g_{\Sigma} = g + d$  with the unique solution  $g_{\Sigma} = 0$ . One can conclude that for a given input



$m = m(\beta, \gamma)$  and  $a = a(\beta, \gamma)$  the final and entirely general form of the  $N = 2$  observable reads

$$\Lambda = \Lambda(D, b, c, g) = \frac{1}{a} \cdot \begin{bmatrix} D a - b - c + i g a, & g - b m + i b a \\ g + c m + i c a, & D a - i g a \end{bmatrix}. \quad (16)$$

We can check that our original Hamiltonian is reobtained at  $D = 2$  (i.e.,  $G = 2$ ),  $b = c = 0$  (i.e.,  $B = C = -1$ ) and  $g = -a$  ( $= -d$ ).

In Ref. [14] the authors recommended to proceed in an opposite direction and select a few matrices (or operators)  $\Lambda_1, \Lambda_2, \dots$  of observables in advance (say, on some fitting or phenomenological grounds). Naturally, these input matrices must necessarily be self-adjoint in  $\mathcal{H}^{(S)}$ , i.e., in our  $N = 2$  example, proportional to our general formula (16). Thus, in the generic case, the series of the necessary cryptohermiticity conditions will, sooner or later, specify all of the values of the free parameters in the metric (up to the above-mentioned trivial rescaling of course).

### 5.3 The concept of charge

In the so called  $\mathcal{PT}$ -symmetric quantum mechanics [2] one introduces an additional requirement which may be mathematically interpreted as the assumption of the Hermiticity of the Hamiltonian in a suitable Krein space [6, 27]. Formally speaking, one just preselects an indefinite Krein-space metric  $\mathcal{P}$  with the property  $\mathcal{P}^2 = I$  (called, conventionally, “parity”). One then postulates the following indefinite-metric parallel of Eq. (10),

$$[H]^\dagger \mathcal{P} = \mathcal{P} H. \quad (17)$$

The main benefit of such an auxiliary assumption is seen in the possibility of the construction of a special and *unique* metric  $\Theta^{(\mathcal{CPT})} = \mathcal{C}\mathcal{P}$  called  $\mathcal{CPT}$  metric. The new operator  $\mathcal{C}$  with property  $\mathcal{C}^2 = I$  is being interpreted as a charge [28].

Our present toy-model Hamiltonian matrices  $H = H^{(N)}(a, z)$  satisfy Eq. (17) with the Hamiltonian-independent matrices of parity  $\mathcal{P} = \mathcal{P}^{(N)}$  containing just the unit elements along the secondary diagonal (i.e.,  $\mathcal{P}_{m,n}^{(N)} = 1$  iff  $m + n = N + 1$  while  $\mathcal{P}_{m,n}^{(N)} = 0$  otherwise). Thus, at  $N = 2$  one could treat  $\mathcal{P}^{(2)}$  as an indefinite limit of  $\Theta [H^{(2)}(a)]$  with  $k^{(\mathcal{P})} \rightarrow 0$  while  $m^{(\mathcal{P})} \rightarrow \infty$  and  $k^{(\mathcal{P})} m^{(\mathcal{P})} \rightarrow 1$ . From the factorization requirement  $\Theta^{(\mathcal{CPT})} = \mathcal{C}\mathcal{P}$  we may eliminate the complex charge

$$\mathcal{C} = \Theta [H^{(2)}(a)]_{(k,m)} \mathcal{P}^{(2)} = \begin{bmatrix} u & v \\ y & z \end{bmatrix} \quad (18)$$

and get  $v = y = k$  and  $z = u^* = k e^{i\gamma} \cos \beta$  (cf. Eq. (13)). The  $N = 2$  version of condition  $\mathcal{C}^2 = I$  requires not only that  $\gamma = \gamma^{(\mathcal{CPT})} = \pi/2$  (i.e., that  $a = \cos \beta$ ) but also that  $\beta = \beta^{(\mathcal{CPT})}$  is such that  $\sin \beta^{(\mathcal{CPT})} = 1/k$ . The resulting metric is unique and we have the unique charge

$$\mathcal{C}^{(\mathcal{CPT})} = k \cdot \begin{bmatrix} -ia & 1 \\ 1 & ia \end{bmatrix}. \quad (19)$$

The comparison of this formula with the general specification of an observable (16) reveals that the charge is an observable in which  $D = b = c = 0$  and  $g = -\cos \beta / \sin \beta = -\sqrt{k^2 - 1}$ .

## 6 The first nontrivial $N = 4$ model

### 6.1 The complete set of pseudometrics

The general four-parametric Hermitian  $N = 4$  candidates for the metric (= “pseudometrics”) may be obtained, most easily, from Eq. (10) again. These solutions appear symmetric with respect to their second diagonal. They may be written in the closed four-parametric form of matrix  $\Theta [H^{(4)}(a, z)]_{(k,m,r,h)} =$

$$= \begin{bmatrix} k & m - ikw & W^* & Z^* \\ m + ikw & r & h - i(kw + ra) & W^* \\ W & h + i(kw + ra) & r & m - ikw \\ Z & W & m + ikw & k \end{bmatrix} \quad (20)$$

where we introduced function  $w = w(z, a) = 3^z a$  (this quantity must be positive and, for  $z > 0$ , larger than  $a$ ) and where we abbreviated

$$W = W(k, m, r) = -w^2 k + r - k - kwa + i(wm + ma) ,$$

$$Z = Z(k, m, r, h) = ma^2 - w^2 m - m + h - i(kw - ka - kwa^2 - rw + w^3 k) .$$

This result seems to indicate that the above-noticed full-matrix structure of the  $N = 2$  metrics will survive the transition to any dimension. Our present choice of the discrete but strictly *local* non-Hermitian interactions  $V(x_j)$  only seems to admit the non-band-matrix, strongly nonlocal forms of *all* of the Hermitizing metrics.

### 6.2 The condition of positivity

Although an immediate correspondence between the above-displayed general  $N = 4$  pseudometric with the most common and usual metric  $\Theta = I$  seems out of question, we may still select, for illustration purposes, the unit main diagonal in formula (20),  $k = r = 1$ . Once we also put  $m = h = 0$  (leading to the simplified elements  $W(1, 0, 1) = -w(w + a)$  and  $Z(1, 0, 1, 0) = i(a + wa^2 - w^3)$ ), we may immediately (and non-numerically) test the positivity of the matrix.

This test may proceed via an immediate evaluation of the four eigenvalues  $\theta_{\pm}^{\pm}$  of the candidate matrix  $\Theta [H^{(4)}(a, z)]_{(1,0,1,0)}$  in the respective closed forms

$$\theta_{+}^{\pm} = 1 + \frac{1}{2} (w - a^2 w + w^3) \pm \frac{1}{2} \sqrt{\Delta^{+}}$$

and

$$\theta_{-}^{\pm} = 1 - \frac{1}{2} (w - a^2 w + w^3) \pm \frac{1}{2} \sqrt{\Delta^{-}}$$

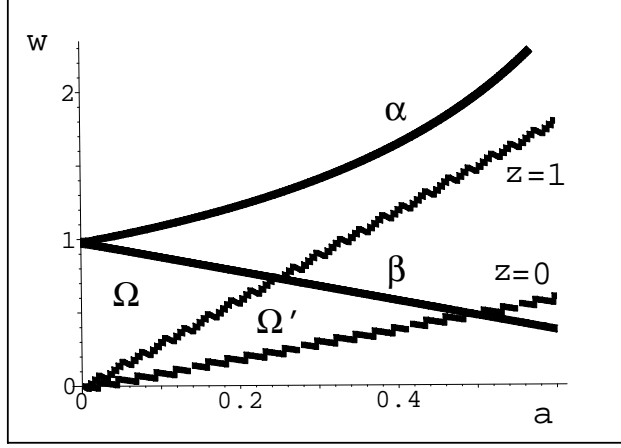


Figure 15: The thick-line upper boundaries  $\alpha = \alpha(a)$  and  $\beta = \beta(a)$  of the respective positivity domains of the respective eigenvalues  $\theta_{\pm}^{+}$  and  $\theta_{\pm}^{-}$  of the eligible metric  $\Theta [H^{(4)}(a, z)]_{(1,0,1,0)}$ .

with the common discriminant

$$\begin{aligned} \Delta^{\pm} = & w^6 + (2 - 2a^2)w^4 + (\pm 8 + 4a)w^3 + (5 \pm 8a + 6a^2 + a^4)w^2 + \\ & + (4a + 4a^3)w + 4a^2. \end{aligned}$$

These formulae enable us to specify the parametric domain of the necessary positivity of the metric  $\Theta [H^{(4)}(a, z)]_{(1,0,1,0)}$  by elementary means.

The results are sampled in Fig. 15 where we displayed the part of the  $(z, a)$  plane where  $\theta_{\pm}^{+} > 0$  so that just the two eigenvalues may get non-positive there. The inspection of this picture enables us to conclude that these eigenvalues remain positive (so that the general pseudometric  $\Theta [H^{(4)}(a, z)]_{(1,0,1,0)}$  becomes tractable as the *positive definite* metric) in the triangular domain  $\Omega \cup \Omega'$  (assuming that  $z > 0$ ) or  $\Omega$  (assuming that  $z > 1$ ). Such a simplification follows from the fact that at the two sample values of  $z = 0$  and of  $z = 1$ , the auxiliary wiggly lines just “translate” the  $a$ -dependence into  $w$ -dependence of the change-of-sign boundary since the auxiliary functions  $w = w(z, a) = 3^z a$  (which enter the above closed formulae as abbreviations) are linear in  $a$ .

## 7 The $N = 6$ model

For the not too large matrix dimensions  $N = 2K$  the technique of the construction of the general pseudometrics  $\Theta$  via the solution of the linear algebraic Eq. (10) remains feasible and straightforward. With the growth of  $N$  the only difficulty emerges in connection with the printed presentation of the resulting multiparametric set of pseudometrics. For this reason it makes sense to find a sufficiently representative set of a few key parameters. For each such choice, moreover, it becomes necessary to determine a boundary of the domain  $\mathcal{D}$  of these key parameters, inside which the pseudometric in

question remains positive definite and, hence, eligible as a metric in a certain “optimal” physical Hilbert space  $\mathcal{H}^{(S)}$ .

In our present setting the task is slightly simplified by the fact that the most relevant values of our first, “kinematical input” parameter  $a$  may be expected small and admitting, therefore, the use of perturbation approximations. Secondly, we may take the variability of the second, “dynamical input” parameter  $z$  for granted. Nevertheless, as long as the choice of this exponent will be mostly dictated by applications (controlling, e.g., the loss of stability of certain most fragile levels), its choice proves not too essential in our present methodical considerations. We shall often consider the “discrete square-well value” [29]  $z = 0$  as a sufficiently instructive and generic option.

## 7.1 The metric at $z = 0$

Even when we set our “methodically redundant” exponent  $z$  equal to zero, we cannot parallel Eq. (20) and display the whole six-parametric matrix  $\Theta$  resulting from the computer-assisted non-numerical solution of Eq. (10). For this reason we further employed the simplification used in subsection 6.2 and demanded that all the elements of the main diagonal of our special  $\Theta$  are chosen equal to one. Although the resulting pseudometric still did not fit in the printed page, the separate matrix elements do and remain sufficiently compact,

$$\begin{aligned}\Theta_{2,1} = \Theta_{6,5} &= m + ia, & \Theta_{3,2} = \Theta_{5,4} &= 4ma^2 + m + d + 2ia, \\ \Theta_{4,3} &= d + 4ma^2 + m + r + 3ia, \\ \Theta_{3,1} = \Theta_{6,4} &= -2a^2 + 2ima, & \Theta_{4,2} = \Theta_{5,3} &= -6a^2 - i(-8ma^3 - 4ma - 2da), \\ \Theta_{4,1} = \Theta_{6,3} &= d - i(4a^3 - a), & \Theta_{5,2} &= r + d - i(-2a + 4a^3), \\ \Theta_{5,1} = \Theta_{6,2} &= -4a^2 - i(-2ma - 8ma^3 - 2da), & \Theta_{6,1} &= r + ia.\end{aligned}$$

The complex conjugates of these elements form the upper-triangle part of  $\Theta = \Theta^\dagger$  of course.

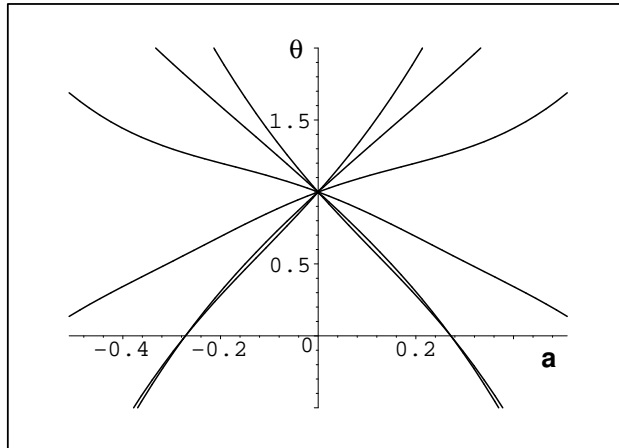


Figure 16: The spectrum of the simplified metric (21).

In a continuation of the search of parallels with the results of subsection 6.2 we may further set  $m = d = r = 0$  and obtain  $\Theta = \Theta_0^{(6)}(a)$  as the sufficiently compact matrix

$$\begin{bmatrix} 1 & -ia & -2a^2 & i(4a^3 - a) & -4a^2 & -ia \\ ia & 1 & -2ia & -6a^2 & i(4a^3 - 2a) & -4a^2 \\ -2a^2 & 2ia & 1 & -3ia & -6a^2 & i(4a^3 - a) \\ i(a - 4a^3) & -6a^2 & 3ia & 1 & -2ia & -2a^2 \\ -4a^2 & i(2a - 4a^3) & -6a^2 & 2ia & 1 & -ia \\ ia & -4a^2 & i(a - 4a^3) & -2a^2 & ia & 1 \end{bmatrix}. \quad (21)$$

The graph of its eigenvalues is displayed in Fig. 16, showing that such a matrix may serve as a metric in Hilbert space iff  $a \in (-\beta^{(6)}, \beta^{(6)})$  with  $\beta^{(6)} \approx 0.2718445$ .

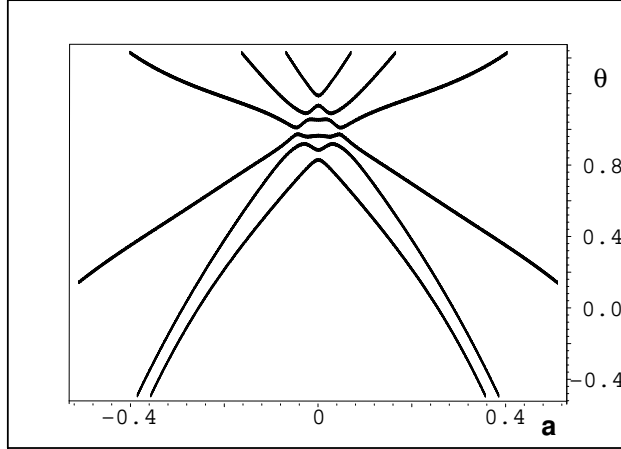


Figure 17: The spectrum of the perturbed metric (21) with  $m = 1/10$ .

The inspection of Fig. 16 reveals that in the domain of very small  $a$ s the  $a$ -dependence of the eigenvalues  $\theta_j(a)$  of the metric  $\Theta_0^{(6)}(a) > 0$  may be very well approximated by the linear functions,  $\theta_j(a) \approx 1 + h_j a$ . The determination of the coefficients  $h_j$  is still easy since we may Taylor-expand the metric

$$\Theta(a) = I + \begin{bmatrix} 0 & -ia & 0 & -ia & 0 & -ia \\ ia & 0 & -2ia & 0 & -2ia & 0 \\ 0 & 2ia & 0 & -3ia & 0 & -ia \\ ia & 0 & 3ia & 0 & -2ia & 0 \\ 0 & 2ia & 0 & 2ia & 0 & -ia \\ ia & 0 & ia & 0 & ia & 0 \end{bmatrix} + \mathcal{O}(a^2) \quad (22)$$

and arrive at the virtually trivial leading-order secular equation

$$h_j^6 - 26h_j^4 + 181h_j^2 - 225 = (h_j^3 - 2h_j^2 - 11h_j + 15)(h_j^3 + 2h_j^2 - 11h_j - 15) = 0$$

and roots  $h_{1,6} = \mp 3.102940862$ ,  $h_{2,5} = \pm 1.256913500$ ,  $h_{3,4} = \pm 3.846027361$ .

The practical use of such a result may be twofold:

- we may assure ourselves that the decrease of the lowest eigenvalue  $\theta_{j_{\min}}(a) \approx 1 - 3.846 a$  *guarantees* that the maximal admissible value of  $a$  is  $\beta \approx 1/3.846027361 \approx 0.2600$  plus/minus  $\mathcal{O}(a^2)$  corrections; this estimate seems fully consistent with the above-derived exact value of  $\beta^{(6)} \approx 0.2718445$ ;
- alternatively, we may restrict ourselves to a much smaller subinterval of  $a$  in which the exact minimal eigenvalue  $\theta_{j_{\min}}(a)$  remains safely positive, say, on the grounds of a variational estimate of corrections (keeping also in mind that  $\max a^2 \approx 0.06$ ).

The formalism of perturbation expansions may be recalled and used to reflect the influence of further parameters. The importance of the possible changes of the spectrum of the metric is sampled in Fig. 17 where the differences from Fig. 16 are all caused by the choice of  $m = 1/10$ . One witnesses the complete removal of the full zero-order degeneracy of the “unperturbed”  $\theta_j = 1 + \mathcal{O}(a)$ . Just a partial removal of the degeneracy may result from the alternative choices, e.g., of  $r \neq 0$  which just splits the six-times degenerate  $a = 0$  eigenvalue  $\theta_j$  in two three-times degenerate descendants.

## 8 Extrapolations and models with $N \geq 8$

At any dimension  $N = 2K$  the dynamical contents of our toy models is controlled by the Hamiltonian (which varies with the “kinematical” parameter  $a \in (-\alpha^{(N)}, \alpha^{(N)})$ , “dynamical” parameter  $z \in (-\infty, \infty)$  and real spectral locus  $\{\varepsilon_j(a, z)\}$ ) and by the Hermitian, positive-definite metric  $\Theta^{(N)}$  specified by an  $N$ -plet of parameters  $\{k, m, \dots\} \in \mathcal{D}$ .

Naturally, practical implementations of such a recipe will require also a determination of the whole positivity domain  $\mathcal{D}$ , or of its suitable non-empty subdomain at least. This task will certainly be facilitated by the smallness of  $a$  in practice. In our constructions performed at  $N \leq 6$  we saw, moreover, that many of the closed small- $a$  formulae might be potentially extrapolated to an arbitrary dimension  $N = 2K$ .

### 8.1 The $N \geq 8$ metrics

One of the most promising keys to the extension of at least some of our above-listed low-dimensional results to all  $N$  has been found in the compact form of the matrix elements of the pseudometrics at  $N \leq 6$ . Indeed, we succeeded in transmuting these small- $K$  elements into larger- $K$  ansatzs and found out that such a method of construction appeared very efficient and quick.

One of the main shortcomings of such a recipe lies in the enormous growth of the size of the formulae caused, mainly, by the linear growth of the number of free parameters with the increasing dimension  $N = 2K$ . This means that in the computer-assisted environment we may still deduce the form

of the  $N$ -parametric pseudometrics  $\Theta^{(N)}$  (from Eq. (10)) but the resulting extrapolations of the above-displayed compact  $K = 1$ ,  $K = 2$  and  $K = 3$  formulae cease to be compact. Thus, for presentation purposes, the majority of the available  $N \geq 8$  results still has to be compactified and transformed, typically, into a graph or numerical table.

During the computer-assisted  $N \geq 8$  constructions themselves, the most difficult obstacle has been found, as we already indicated, in the necessary specification of the boundaries of a non-empty metric-positivity (sub)domain  $\mathcal{D}^{(N)}$ . Fortunately, the very natural assumption of smallness of  $a$  almost trivialized the problem at  $N \leq 6$  and proved also helpful at the higher dimensions. The point was that the advantage of the practical negligibility of  $a^2$  shortened the solution of Eq. (10), implying the – unexpected – easiness of the extrapolation of the matrix elements of pseudometrics to all  $N$ .

As we have already noted, the complete, multiparametric matrices  $\Theta$  can hardly be displayed, in print, even at  $K = 3$ . For this reason, let us restrict our attention to certain special subsets of metrics and present the theory “via examples”. Firstly, let us skip the questions of energies (discussed, at length, in the preceding sections after all) and study, from now on, just the simplest possible toy-model dynamics with  $z = 0$ .

Secondly, let us circumvent the (difficult) problem of the determination of the exact “exceptional point” boundaries  $\partial\mathcal{D}^{(N)}$  (redirecting the interested readers, say, to our dedicated study [30]) and let us select just a single representative point (i.e., multiindex  $\mu := (k, m, \dots) \rightarrow (k_0, m_0, \dots) := \mu_0$ ) which lies safely inside the hypothetical parametric domain  $\mathcal{D}^{(N)}$ .

Thirdly, the guarantee of the latter requirement  $\mu_0 \in \mathcal{D}^{(N)}$  will be made easy via the extension of our previous  $N \leq 6$  experience to all  $N$  and by the selection of the main-diagonal elements of the candidate for the metric equal strictly to one,  $\Theta_{n,n} = 1$ ,  $n = 1, 2, \dots, N$  (i.e.,  $k_0 = 1, \dots$ ), with all of the other parameters staying “sufficiently small” (i.e.,  $|m_0| \ll 1, \dots$ ).

## 8.2 The $N \geq 8$ metrics at $z = 0$ and at small $a$

In a continuation of our simplified presentation of the extrapolation ideas let us now select the dimension  $N = 8$  and set all of the “small” parameters in a general pseudometric  $\Theta$  strictly equal to zero (i.e.,  $m_0 = 0, \dots$ ). Immediately, the explicit solution of Eq. (10) will generate the pseudometric  $\Theta_0^{(8)}$  with matrix elements which become predictable, by extrapolation, from their above-displayed  $N = 6$  predecessors.

On this basis we verified, numerically, that also the  $a$ -dependence of the spectrum  $\{\theta_j\}$  of the new pseudometric  $\Theta_0^{(8)}(a)$  remains very similar to the one sampled in Fig. 16 above. We deduced, extrapolated and also re-verified at  $N = 10$  that at any  $N = 2K$ , one may expect and conjecture to see the  $K$ -plet of curves  $\theta_j(a)$  which are moving quickly up with the growth of  $|a|$ , complemented by another  $K$ -plet of curves  $\theta_j(a)$  which are moving quickly down with the growth of  $|a|$ .

At this moment one can recollect the  $N = 6$  discussion of Fig. 16 and formulate the following two questions concerning the determination of the pseudometric-positivity interval of  $a \in (-\beta^{(N)}, \beta^{(N)})$  at the general dimen-

sion:

- do the left and right intersections  $\pm\beta^{(N)} \in \partial\mathcal{D}^{(N)}$  of the lowest eigenvalue curve  $\theta_{j_{\min}}(a)$  with the  $a$ -axis leave a non-empty and/or sufficiently large space for the variability of  $a$  at large  $N = 2K$ ?
- would the linear approximation  $\theta_{j_{\min}}(a) = 1 + h_{j_{\min}} a$  of the minimal eigenvalues provide a sufficiently reliable estimate of the exact exception-point values of  $\beta^{(N)}$ ?

Whenever both of the answers happen to be positive, we may proceed further, accept the above-introduced perturbation-approximation philosophy and linearize our pseudometric. Thus, we returned to Eq. (10), constructed the linearized matrix  $\Theta_0^{(8)}$  and obtained it in the following, very regular sparse-matrix form

$$\begin{bmatrix} 1 & -ia & 0 & -ia & 0 & -ia & 0 & -ia \\ ia & 1 & -2ia & 0 & -2ia & 0 & -2ia & 0 \\ 0 & 2ia & 1 & -3ia & 0 & -3ia & 0 & -ia \\ ia & 0 & 3ia & 1 & -4ia & 0 & -2ia & 0 \\ 0 & 2ia & 0 & 4ia & 1 & -3ia & 0 & -ia \\ ia & 0 & 3ia & 0 & 3ia & 1 & -2ia & 0 \\ 0 & 2ia & 0 & 2ia & 0 & 2ia & 1 & -ia \\ ia & 0 & ia & 0 & ia & 0 & ia & 1 \end{bmatrix}.$$

We see that the extrapolation of this leading-order form of the pseudometric to any  $N = 2K$  is truly trivial. Also the construction of its linear-approximation eigenvalues  $\theta_j(a) = 1 + h_j a$  remains feasible at any dimension. For illustration let us just select  $N = 8$  and display the related leading-order secular equation for the coefficients,

$$h_j^8 - 70 h_j^6 + 1487 h_j^4 - 9139 h_j^2 + 11025 = 0.$$

It may again be factorized yielding the two parallel rules

$$h_j^4 \mp 2 h_j^3 - 33 h_j^2 \pm 47 h_j + 105 = 0$$

and roots 1.259204635, 2.752948888, 5.256297172 and 5.762552919 of both signs which determine the leading-order eight-line-crossing small- $a$  part of the  $N = 8$  analogue of the  $N = 6$  spectra of Fig. 16.

We may add that the linear-extrapolation prediction  $1/5.76255 \approx 0.1735$  of the exceptional-point value as obtained from the maximal root again compares very well with the exact numerical value of  $\beta^{(8)} \approx 0.1683983$ . Thus, the linear approximation leads to the error  $\sim 0.005$  which happens to be much smaller than the rough estimate  $\sim [\beta^{(8)}]^2 \approx 0.03$  of the typical magnitude of the second order correction.



### 8.3 Discussion: the $N \geq 8$ discrete approximants and an efficient spectral design

Our present proposal of working with discrete, matrix quantum models of finite dimension has been initiated by certain formal difficulties encountered, in the literature, during the attempted assignments of a nontrivial Hilbert-space metric to a given, non-Hermitian differential Hamiltonian operator possessing the strictly real spectrum. Typically, these difficulties are being circumvented via additional assumptions (cf. our comments above, especially in section 2).

During the very initial step of our analysis (viz., during the replacement of Eq. (1) by Eq. (4) using a finite number of grid points  $N = 2K$ ) an elementary parameter  $a$  emerged and specified a fixed length in our models. In comparison with the differential-operator predecessors of our models, a new quality emerged since the spectra of energies became “fragile”, i.e., complex beyond a certain critical kinematics-related size-parameter  $a_{critical} = \alpha^{(N)} > 0$ .

From the point of view of the variability of dynamics our initial choice of the one-parametric discrete versions of the very special potential of the imaginary cubic oscillator (as made in section 3) did not prove too satisfactory. Fortunately, we managed to shift the role of the most unstable state to optional excitations by means of a re-scaling of the potential based on an introduction of another, “dynamical” exponent-parameter  $z \in \mathbb{R}$ .

Undoubtedly, the latter trick made the structure (and, in particular, the “topological menu”) of the energy levels “universal” in the sense illustrated, at  $N = 8$ , in Table 2. At the same time, the mechanism of the changes of the topological structure of the spectral loci  $\varepsilon_j(a)$  remained transparent and tractable, schematically, as an up and down “motion” of the two (deformed) circles. In this context the information compressed in Table 2 was complemented, graphically, by a series of illustrative pictures. All of these observations will find their strict analogues at any integer  $N = 2K$ .

Another merit of our toy-model simulations of dynamics may be seen in the related feasibility of the constructions and in the extrapolation-friendliness of the multiparametric matrices of the pseudometrics. This implies, certainly, the rarely encountered and equally rarely employed freedom of the control of dynamics by the metric and of the related, rarely emphasized [14] theoretical possibility of the *ad hoc* modifications of the classes of the additional observables  $\Lambda_1, \Lambda_2, \dots$

An important further merit of our present models has been found in the feasibility of the computer-assisted generation and *extrapolations* of important formulae (as well as of their graphical pendants and topological interpretations) *to all*  $N$ . As an immediate consequence one must appreciate, among others, the facilitated estimates of the ranges of the positivity of the pseudometrics, or the facilitation of the applicability of the linear-algebraic and perturbation-expansion techniques.

Many of these ideas may find further applications. At the same time, we would expect that in the spirit, say, of Refs. [31, 32], the next-step developments of the subject should be aimed at the simulations of dynamics which replace the local potentials  $V(x)$  by some slightly non-local generalizations.

Also in this respect, the present technique of discretization may be expected to lower many purely technical obstacles.

## 9 Summary

Our first tests of the idea of discretization proved disappointing. We observed that the growing-dimension series (7) of the simple-minded one-parametric descendants of the popular differential imaginary cubic oscillator do not offer a sufficiently rich variability of the coupling-dependence of the energy spectra. Fortunately, the merely slightly more sophisticated and re-scaled two-parametric choice (8) of the model has been shown to offer a flexibility of the spectral loci which covers a broad menu of alternative mechanisms of the phenomenologically interesting tunability.

In our two-parametric model the breakdown of stability of the system was shown to be caused by the spontaneous, dynamically controlled complexification which could be designed as destroying the reality and stability of any pre-selected pair of neighboring bound states.

The price to be paid for such a highly welcome universality of the model lies in the necessity of a rather complicated construction of the physical *ad hoc* metrics  $\Theta$ . In this setting we took the advantage of the efficiency of the direct solution of the Dieudonné’s Eq. (10) as reported in Ref. [31]. We discussed the related idea of reduction of the ambiguity of the metric via the requirement of its maximal computational friendliness, i.e., of its sparse-matrix structure. We tested this possibility and arrived at encouraging results here.

One of the main formal advantages of our present class of models may be seen in the possibility of its detailed study at the smallest dimensions followed by the formulation of ansatzs and by their tests and successful trial-and-error extrapolations to *arbitrary* dimensions. A particularly efficient application of such a strategy has been found in the context of perturbation-series constructions where we made use of the fact that due to its Runge-Kutta-approximation origin, the parameter  $a$  may be truly considered very small in practice.

Our analysis also confirmed expectations that for the real exponents  $z$ , the metric operators can never be diagonal or banded matrices. This seems to be a characteristic consequence of the choice of a local form of the interaction for which the inner products remain “long-ranged” in the sense explained, in the context of scattering theory, by Jones [20]. Thus, in accord with our commentary in [19] we believe that the requirement of the unitarity of the scattering implies the necessity of introduction of at least small non-localities in the interaction. In opposite direction we expect that our present complex local-like Hamiltonians will preserve the analogy with their differential-operator-like  $N \gg 1$  limits. In particular, we are persuaded (and would like to conjecture) that these models of dynamics will never admit the existence of a unitary and causal version of the scattering, not even in the “short-range” dynamical regime with very negative exponents  $z \ll 0$ .

# Acknowledgements

Work supported by the GAČR grant Nr. P203/11/1433, by the MŠMT “Doppler Institute” project Nr. LC06002 and by the Institutional Research Plan AV0Z10480505.

# References

- [1] P. Dorey, C. Dunning and R. Tateo, J. Phys. A: Math. Theor. 40, R205 (2007).
- [2] C. M. Bender, Rep. Prog. Phys. 70, 947 (2007).
- [3] A. Mostafazadeh, Int. J. Geom. Meth. Mod. Phys. 7, 1191 (2010).
- [4] M. Znojil, SIGMA 5, 001 (2009).
- [5] M. Znojil, J. Math. Phys. 45, 4418 (2004);  
M. Znojil, Phys. Lett. B 647, 225 (2007);  
Y. N. Joglekar, D. Scott, M. Babbey and A. Saxena, Phys. Rev. A 82, 030103(R) (2010);  
A. Cavaglia, A. Fring and B. Bagchi, J. Phys. A: Mat. Theor. 44, 325201 (2011);  
H. Schomerus, Phys. Rev. A 83, 030101(R) (2011);  
Y. N. Joglekar and J. L. Barnett, arXiv:1108.6083.
- [6] H. Langer and Ch. Tretter, Czechosl. J. Phys. 70, 1113 (2004).
- [7] E. Caliceti, S. Graffi and M. Maioli, Commun. Math. Phys. 75, 51 (1980).
- [8] G. Alvarez, J. Phys. A: Math. Gen. 27, 4589 (1995).
- [9] C. M. Bender and K. A. Milton, Phys. Rev. D 55, R3255 (1997).
- [10] C. M. Bender and S. Boettcher, Phys. Rev. Lett. 80, 5243 (1998).
- [11] E. Delabaere and D. T. Trinh, J. Phys. A: Math. Gen. 33, 8771 (2000);  
M. Znojil, Phys. Lett. A 374, 807 (2010);  
J. Zinn-Justin and U. Jentschura, J. Phys. A: Math. Theor. 43, 425301 (2010).
- [12] P. Dorey, C. Dunning and R. Tateo, J. Phys. A: Math. Gen. 34, 5679 (2001).
- [13] G. Lévai and M. Znojil, J. Phys. A: Math. Gen. 33, 7165 (2000);  
G. Lévai, A. Sinha and P. Roy, J. Phys. A: Math. Gen. 36, 7611 (2003).
- [14] F. G. Scholtz, H. B. Geyer and F. J. W. Hahne, Ann. Phys. (NY) 213, 74 (1992).

- [15] C. M. Bender, P. N. Meisinger and Q. Wang, J. Phys. A: Math. Gen. 36, 1973 (2003).
- [16] C. M. Bender, D. C. Brody, and H. F. Jones, Phys. Rev. D 70, 025001 (2004).
- [17] M. Znojil, SIGMA 4, 001 (2008).
- [18] A. Mostafazadeh, J. Phys. A: Math. Gen. 39, 10171 (2006).
- [19] M. Znojil, J. Phys. A: Math. Theor. 41, 292002 (2008); Phys. Rev. D 78, 025026 (2008) and Phys. Rev. D 80, 045009 (2009).
- [20] H. F. Jones, Phys. Rev. D 78, 065032 (2008).
- [21] M. Znojil, SIGMA 5, 085 (2009).
- [22] M. Znojil, J. Phys. A: Math. Theor. 43, 335303 (2010).
- [23] M. Znojil, Phys. Lett. A 375, 3435 (2011).
- [24] M. Znojil, SIGMA 7, 018 (2011).
- [25] P. K. Ghosh, Int. J. Theor. Phys. 50, 1143 (2011).
- [26] J. Dieudonne, Proc. Int. Symp. Lin. Spaces (Pergamon, Oxford, 1961), p. 115.  
J. P. Williams, Proc. Amer. Math. Soc. 20, 121 (1969).
- [27] I. C. Gohberg and M. G. Krein, Introduction to the Theory of Linear Nonselfadjoint Operators. Translations of Mathematical Monographs 18, American Mathematical Society, Providence, RI, 1969;  
E. B. Davies, Linear operators and their spectra. Cambridge University Press, Cambridge, 2007;  
J.-P. Gazeau, P. Siegl, and A. Youssef, SIGMA, 6 (2010).
- [28] C. M. Bender, D. C. Brody and H. F. Jones, Phys. Rev. Lett. 89, 270401 (2002).
- [29] M. Znojil, J. Phys. A: Math. Gen. 39, 10247 (2006).
- [30] M. Znojil, J. Phys. A: Math. Theor. 40, 4863 (2007); J. Phys. A: Math. Theor. 40, 13131 (2007) and J. Phys. A: Math. Theor. 41, 244027 (2008).
- [31] M. Znojil, Phys. Rev. D 80, 045022 (2009) and Phys. Rev. D. 80, 105004 (2009).
- [32] P. E. G. Assis and A. Fring, J. Phys. A: Math. Theor. 42, 015203 (2009).